Published in final edited form as:
Brain Res Mol Brain Res. 2005 May 20; 136(1-2): 164–176.

From synapse to gene product: Prolonged expression of c-*fos* induced by a single microinjection of carbachol in the pontomesencephalic tegmentum

James J. Quattrochi[a,*], **Mihaela Bazalakova**[a,1], and **J. Allan Hobson**[b]
a*Laboratory for Cellular and Molecular Neuroscience and Program in Neuroscience, Harvard Medical School, WAB 425/447B, 200 Longwood, Boston, MA 02115, USA*

b*Laboratory of Neurophysiology, Harvard Medical School, Boston, MA 02115, USA*

Abstract

It is not known how the brain modifies its regulatory systems in response to the application of a drug, especially over the long term of weeks and months. We have developed a model system approach to this question by manipulating cholinergic cell groups of the laterodorsal and pedunculopontine tegmental (LDT/PPT) nuclei in the pontomesencephalic tegmentum (PMT), which are known to be actively involved in the timing and quantity of rapid eye movement (REM) sleep. In a freely moving feline model, a single microinjection of the cholinergic agonist carbachol conjugated to a latex nanosphere delivery system into the caudolateral PMT elicits a long-term enhancement of one distinguishing phasic event of REM sleep, ponto-geniculo-occipital (PGO) waves, lasting 5 days but without any significant change in REM sleep or other behavioral state. Here, we test the hypothesis that cholinergic activation within the caudolateral PMT alters the postsynaptic excitability of the PGO network, stimulating the prolonged expression of c-*fos* that underlies this long-term PGO enhancement (LTPE) effect. Using quantitative Fos immunohistochemistry, we found that the number of Fos-immunoreactive (Fos-IR) neurons surrounding the caudolateral PMT injection site decreased sharply by postcarbachol day 03, while the number of Fos-IR neurons in the more rostral LDT/PPT increased >30-fold and remained at a high level following the course of LTPE. These results demonstrate a sustained c-*fos* expression in response to pharmacological stimulation of the brain and suggest that carbachol's acute effects induce LTPE via cholinergic receptors, with subsequent transsynaptic activation of the LDT/PPT maintaining the LTPE effect.

Keywords

Immediate early gene; c-*fos*; Carbachol nanospheres; Brainstem; Ponto-geniculo-occipital waves; Sleep

1. Introduction

One of the most baffling and fundamental questions in neuroscience concerns how activity-dependent alterations in gene expression regulate long-term behavioral changes and the prolonged time course of such disabling disorders as addiction, depression, and other chronic psychiatric illnesses [22,25,38,39,61]. The ability of drugs to induce a complex pattern of immediate early gene (IEG) expression is thought to be an important first step in producing persistent forms of neurobehavioral plasticity [40,62,74]. The prominence of progressively

*Corresponding author. *E-mail address:* jq@hms.harvard.edu (J.J. Quattrochi).
[1]Present address: Vanderbilt University School of Medicine, Brain Institute and Neuroscience Program, Nashville, TN 37235, USA.

developing and persistent adaptations in brain function may be attributed to long-term changes in the molecular constituents of neurons and, thus, the functional activity of neural circuits in mediating behavioral state. The study of sleep provides an opportunity to investigate the relationship between synaptic events and possible downstream molecular alterations in these long-term behavioral phenomena. Here we take advantage of our recent discovery that certain rapid eye movement (REM) sleep events can be dissociated from the rest of the REM behavioral state to investigate how acute, local synaptic events in one part of the brain can trigger long-term alterations in expression of gene product at remote sites.

The pontomesencephalic tegmentum (PMT) was first shown to be critical for the generation of REM sleep in early studies using transection and lesion techniques [24,88]. Pharmacological evidence subsequently indicated that acetylcholine is important for the timing and quantity of REM [2] and that the Ch5 and Ch6 cholinergic cell groups [53] within the PMT are actively involved in the control of REM sleep and the ponto-geniculo-occipital (PGO) waves that are a distinguishing phasic component of REM [7,16]. The objective of the present study is to determine which neurons in the PMT are activated in association with the cholinergically-induced, long-term enhancement of PGO waves.

Microinjection of the cholinergic agonist carbachol into the anterodorsal paramedian pontine reticular formation elicits an immediate increase in REM sleep lasting 4–6 h that is electroencephalographically similar to physiologically normal REM [3,67]. In contrast, a single micro-injection of carbachol into the caudolateral PMT elicits a very different effect of REM sleep enhancement within normal sleep time lasting 6–10 days [18]. Using micro-injections of a carbachol-conjugated latex nanosphere delivery system (LNDS) [46,67] that limits the diffusion of drug at these pontomesencephalic sites, our neuroanatomical studies identified cholinergic and non-cholinergic afferent neurons within the PMT associated with this long-term REM enhancement [68].

We recently reported that a single microinjection of carbachol at sites within the PMT just 0.4 mm rostral to those triggering long-term REM enhancement produces a long-term PGO enhancement (LTPE) lasting 5 days, but without any significant changes in behavioral state, including REM sleep [66]. The functional involvement of the PMT in this cholinergically-induced long-term behavioral response adds a novel finding to the known behavioral and autonomic responses of this pontine region [5,26,43-45,50,69,73].

Expression of c-*fos* has been used extensively as a cellular marker of neuronal activity [56] and has been of particular interest to behavioral neuroscientists investigating sleep–wake state control [8-11,47,52,76,81,82,90]. Moreover, alterations in the expression of transactivating proteins in the brain that influence the transcription of genes involved in long-term changes in behavioral phenotype are well established for the protein products of transcription factor activating protein-1 (AP-1) genes, particularly c-*fos* [36,57,84]. In the present study, we investigated the neuronal expression of Fos-immunoreactive (Fos-IR) protein in order to determine whether cholinergic induction of LTPE is associated with c-*fos* expression in the PMT. These findings are the first demonstration of a sustained, long-term c-*fos* expression in response to pharmacological stimulation of the brain.

2. Materials and methods

This study is based on data from $n = 16$ adult male cats weighing 2.8–3.0 kg and 71,385 analyzed neurons. Animals were used according to an institution-approved protocol.

2.1. Animals and surgical preparation

Animals were surgically implanted under halothane (1–2%) anesthesia with a standard set of chronic bilateral electrodes to record the transcortical electroencephalogram (TCX) placed over the frontoparietal cortices, electromyogram (EMG), electrooculogram (EOG), and PGO wave activity from the lateral geniculate nucleus (LGN). All electroencephalographic (EEG) leads were connected to an Amphenol 33-pin connector plug that was attached to the vertex of the skull with dental acrylic cement. Bilateral stainless steel guide cannulae (26 gauge) were stereotaxically implanted and aimed 5 mm above the injection sites in the caudolateral PMT (P3.6, L4.5, H-2.5) according to Berman [4] and as described previously [68]. A jugular intravenous (iv) catheter was inserted for later anesthesia and perfusion. Butorphanol (0.02–0.05 mg/kg) was administered intramuscularly (im) for postsurgical pain. Approximately 10 days following surgery, cats began a week-long adaptation protocol before experimental trials were begun. This adaptation period included play, exercise, handling, positioning during the microinjection procedure, and familiarity with the unrestrained freely moving recording procedure.

2.2. Sleep–wake physiology and microinjection techniques

Each cat was placed in an electrically shielded, well ventilated, sound-attenuated 4 × 4 × 4 in. recording chamber that was outfitted with a plexiglass viewing window. Animals were attached to a cable/commutator system that permitted them to freely move within the chamber. Water was provided ad libitum, the floor and three sides of the chamber were carpeted, and a litter tray was also provided. A 12-h light/dark cycle and ambient temperature control at 23 °C were maintained in the recording chamber and adjacent housing area. In order to establish baseline values, recordings were performed during 4 consecutive 4-h sessions between 12:00 and 16:00 for each cat. A Grass 78 multichannel polygraph with 7P511 amplifiers and a Grass electroencephalograph (Neurodata Model 15) with 15A54 quad amplifiers, 15 CT controller, and interfaced with an IBM P4 were used to acquire and store digitized data (sampling rate = 333 Hz/channel).

The behavioral states of waking (W), slow wave sleep (SWS), the transition state from SWS to REM (defined as SP with >3 PGO waves/15 s), and REM sleep were assessed and quantified in 15-s epochs by Grass Gamma PSG software and computer-automated scoring [48,49] during each consecutive 4-h recording over 7 days. Bilateral PGO waves were quantified as LGN waveforms with an initial positive deflection from baseline of >150-μV amplitude and at least twice that of background activity followed by an opposite polarity and slower deflection [66].Adata acquisition program effectively measured LGN waveform amplitude units with >93% reliability as previously described [49,66] using period-amplitude criteria for the large positive deflection of a PGO spike. The summed total of PGO wave spikes in SP and REM included cluster type characteristics of type I for singlet PGO spikes, and types II, III, and IV for clusters of 2, 3, and >4 PGO waves, respectively, each with interspike intervals <300 ms [7].

Microinjection procedures consisting of vehicle (unconjugated nanospheres, 0.9% saline) and carbachol-conjugated nanospheres have been detailed previously [67,68]. All microinjections were performed with a 1-μl Hamilton syringe attached to a 31-gauge stainless steel injector cannula 5 mm longer than the implanted guide cannulae and with a tip diameter of 40 μm. Following baseline recordings, each animal received a single microinjection at unilateral sites within the caudolateral PMT lasting 60 s at 12:00 in the unanesthetized awake state. Microinjections consisted of vehicle control (n = 4, 250 nl) and carbachol-conjugated nanospheres (n = 12, 13 μg/250 nl).

2.3. Protocol design

At the end of each 4-h recording session on designated postinjection days 01, 03, 05, and 07, cats were deeply anesthetized with sodium pentobarbital (Nembutal, 50 mg/kg, iv) while remaining undisturbed during sleep in the recording chamber. The time from administration of Nembutal to perfusion was 6–7 min for each cat. In order to assure consistency of protocol design for the study of c-*fos* expression, cats were divided into vehicle control (n =4) and carbachol nanosphere (n = 12) groups, and matched by postinjection hours to perfusion (see Table 1). Although we did not perform vigilance or behavioral testing, no changes in behavior were observed during LTPE [66].

2.4. Histochemical techniques

All cats were perfused transcardially with cold isotonic heparinized (5 mg/kg) saline followed by 10% formalin (Sigma) in 0.1 M phosphate buffer (pH 7.4). Brain tissue was removed, blocked along the rostrocaudal axis, and postfixed in buffered formalin on a slow speed table-top shaker overnight. Transverse sections from the pontine brain stem, midbrain, and hypothalamus were cut at a thickness of 40 μm using a Leica 1000 S vibratome equipped with an ice-cold 0.1 M phosphate buffer bath. Sections were taken in series at 160-μm intervals and processed for Fos immunohistochemistry. Tissue sections were incubated for 48 h at 4 °C in rabbit primary Fos antibody (Ab-5, Oncogene Research Products, 1:120,000 dilution) raised against the N-terminal amino acid region of the protein. Sections were subsequently incubated with biotinylated goat anti-rabbit IgG (Vector Laboratories, 1:1,000 dilution) for 2 h at room temperature. Sections were then incubated using an avidin-biotin complex protocol (ABC Vector Elite, 1:200 dilution) with 3,3′-diaminobenzidine (DAB, 0.04%) as the substrate/chromogen. Sections were mounted onto slides (Super Frost Plus, Fisher Scientific), dehydrated through a series of alcohols, cleared in methyl salicylate and xylene, coverslipped with Fluoromount mountant (Gurr 36098, Gallard-Schlesinger/BDH Laboratories, Dorset, UK), and examined with a Zeiss Axioskop epifluorescence photo-microscope. Control incubations without the primary antibody and in the presence of normal serum were processed simultaneously in selected adjacent sections from each series resulting in no specific Fos nuclear staining.

2.5. Histological analysis of Fos-IR neurons

Fos-IR neurons were examined quantitatively without knowledge of the postinjection time to perfusion, vehicle, or pharmacological effect. The number of Fos-IR neurons was counted ipsilateral and contralateral to the micro-injection site in 17 brain stem and subcortical cell groups from each brain that included the laterodorsal tegmentum nuclei (LDT), pedunculopontine tegmentum nuclei (PPT), parabrachial nuclei (PBN), lateral/medial vestibular nuclei (L/MVN), gigantocellular tegmental field (FTG) of the pontine reticular formation (PRF), dorsal raphe nucleus (DRN), nuclei of the locus coeruleus (LC), central nucleus (CN) of the amygdala, dentate gyrus (DG), CA3, and CA1 of the hippocampus, medial habenula nuclei (MHN), and nuclei of the centromedial (CMN), dorsomedial (DMN), dorsolateral (DLN), and posterolateral (PLN) hypothalamus. For clarity and consistency in the text, the parabrachial nuclear region of the caudolateral PMT is termed PBN, distinguishing this region from the more rostral LDT/PPT nuclei of the PMT.

Fos-IR neurons were delineated by nuclear staining and were computer digitized. Quantification of Fos-IR neurons was performed through the rostrocaudal extent of each cell group from three schematically reconstructed maps of section perimeters and nuclear boundaries at different stereotaxic levels determined by the specific nuclei (A8.0–A10.0 for subnuclei of the posterior hypothalamus and MHN, A1.5–A6.5 for the CN of the amygdala and DG, CA3, CA1 of the hippocampus, and A1.0–P6.0 for nuclei of the pontine brain stem). Sections were examined with brightfield illumination for identification of Fos-IR neurons and

with rhodamine epifluorescence (red fluorophore, 550 nm) for nanosphere injection sites. Immunoreactive cells within the perimeter density zone of serially reconstructed nanosphere injection sites were regarded as “false positives” and were not quantified. Since nonspecific immunohistochemical IEG expression can be observed as a result of stress and handling of the animal, we controlled our protocols for habituation of animals to the recording and microinjection procedures, remote iv administration of Nembutal, postinjection times to perfusion, specificity of antisera, and time course analysis of IEG expression as compared to controls.

Using a 3-D digitization system equipped with a Cool-SNAP CCD camera (Photometrics) and image analysis software (IPLab, Scanalytics), the *x*,*y*,*z* position of each Fos-IR neuron in individual sections and the location of nanosphere injection sites were digitized to an accuracy of 1.0 μm and entered in an image data file. Section outlines and nuclear boundary contours were reconstructed from adjacent sections and displayed with each Fos-IR neuron represented by one circle. Histograms were produced to quantitatively examine the temporal organization and mapping of Fos-IR neurons. The *x*,*y*,*z* position of the nanosphere injection site was examined with respect to section contours and a stereotaxically placed, parasagittal fiducial. The mean diameter of injection sites was calculated from serial digitization and measurement of the minor/major elliptic axes of nanosphere fluorescence.

2.6. Statistical analysis

We calculated the design of the study using Nquery/V4.0 software, and estimated that a sample size of $n = 4$ cats at each postinjection time point of the LTPE effect achieves 90% power. Multiple comparisons of the number of Fos-IR neurons within each cell group were performed between control and carbachol nanosphere groups at each time point during the LTPE effect. Statistical analysis of the data was performed by the Mann–Whitney test with significance at $P < 0.025$ (Bonferroni correction). Ipsilateral and contralateral counts of Fos-IR neurons were averaged per section within each cell group per animal and at each time point. Values are reported as the means ± SEM.

3. Results

We performed a quantitative analysis of the distribution and time course of Fos-IR neurons within selected cell groups at different time points over a period of 7 days following a single unilateral microinjection of carbachol nanospheres in the caudolateral PMT. We emphasize three major findings: (1) during the five postcarbachol days in which the LTPE effect was restricted to the PGO-related sleep states of SP and REM, there was a persistent increase in c-*fos* expression within the PMT that paralleled the intensity and time course of PGO enhancement; (2) on day 01, the number of Fos-IR neurons in the vicinity of the drug injection site increased 24-fold; this peak was followed by a 9-fold decline on day 03 while activity in the more rostral LDT/PPT nuclei and the L/MVN continued to rise and remain high; and (3) on day 03, the number of Fos-IR neurons increased to a dramatic 40-fold peak in the LDT/PPT and L/MVN.

3.1. Carbachol nanosphere-induced LTPE and Fos immunoreactivity

A single unilateral microinjection of carbachol-conjugated nanospheres in the caudolateral PMT elicited LTPE lasting 5 days without any significant change in sleep states or waking. Table 1 shows the percentage of sleep–wake states, the LTPE profile as the number of PGO waves in SP and REM, and postinjection hours to perfusion for microinjections of vehicle ($n = 4$) and carbachol nanospheres ($n = 12$) on days 01, 03, 05, and 07 in all cats in the study.

Pharmacologically effective injection sites that induced LTPE were histologically identified and reconstructed under brightfield illumination and rhodamine epifluorescence in the caudolateral PMT, centered ventral to the inferior medial margin of the brachium conjunctivum measured to a mean radial distance of 50–180 μm (Figs. 1A and B). Compared to injections of free drug [46], LNDS limits 1000-fold the diffusion of carbachol and exerts its acute cholinergic effect within a small and well-defined injection site.

Fig. 1C shows Fos-IR neurons in the PPT cell group of the rostral PMT on day 03. Fos-IR neurons were generally clustered and seen in increased numbers with successive days of LTPE. Plotted as a function of postinjection days of LTPE, the mean number of Fos-IR neurons in the LDT/PPT increased with increasing PGO intensity over the course of LTPE, reaching a 31-fold peak (513.2 ± 30.5) on day 03 (Fig. 1D). The pattern of Fos-IR staining in these cell groups of the PMT reflected the number of PGO wave events and followed the 6-day postinjection time course of LTPE. This time course also reflects previous results describing the evolution of long-term REM enhancement that have been produced by microinjections of carbachol nanospheres at sites more posterior in the PMT [18,68].

3.2. Characteristics of Fos immunoreactivity

Fos immunoreactivity was restricted to the nuclei of cells with variations in the intensity of immunostaining within individual sections even between neighboring cells. Examples of Fos-IR neurons on postcarbachol day 03 are illustrated in the LDT/PPT, PBN, and MVN in Fig. 2. Many Fos-IR neurons were scattered in the LDT (Fig. 2A) and PPT (Fig. 2B); clusters of a few Fos-IR neurons were seen in the PBN (Fig. 2C). Almost no Fos-IR neurons were observed in the paramedian FTG (Fig. 2D) of the PRF, a brain stem region that has been implicated in the modulation of REM sleep.

3.3. Distribution and time course of Fos immunoreactivity within the pontomesencephalic tegmentum

Because of the physiological importance of the PMT as part of the PGO and REM sleep generator networks, we wanted to determine the precise spatial and temporal distribution of Fos-IR neurons during the course of the LTPE effect. A schematic map of the distribution of Fos-IR neurons within specific nuclear regions of the pontine brain stem from one representative control and 4 of the twelve LTPE animals on postcarbachol days 01, 03, 05, and 07 is shown in Fig. 3. In both control and LTPE groups, Fos-IR neurons were distributed in the LDT/PPT, PBN, L/MVN, brachium conjunctivum, periaqueductal nuclei, inferior colliculus, central reticular fasciculus, medial and lateral lemniscus, and pontine gray. A few scattered Fos-IR neurons were also evident in the DRN, nuclei of the raphe pontis and magnus, LC, central tegmental field, paralemniscal tegmental field, FTG, medial longitudinal fasciculus, tegmental reticular nuclei, motor trigeminal nuclei, and medial nucleus of the superior olive. No Fos-IR neurons were seen in the central superior nuclei and ventral tegmentum nuclei.

Day 01 of LTPE showed many more Fos-IR neurons clustered bilaterally within the LDT/PPT, L/MVN, and PBN in the vicinity of the injection site at level P3.6 compared to controls (see arrowhead in Fig. 3). However, on day 03 at the peak of the carbachol-induced PGO enhancement, relatively few Fos-IR neurons were evident at the injection site. Furthermore, these neurons were largely confined to levels P3.0–4.0. Fos-IR neurons persisted in the L/MVN at level P5.0 and further increased in number within the LDT/PPT for over 48 h following the single microinjection of carbachol on day 01, which indicates that these rostral cell groups of the PMT continue to be active during LTPE. On day 05, many Fos-IR neurons continued to persist in the PMT. On day 07, the number of Fos-IR neurons approximated controls and the PGO enhancement effect returned to baseline.

Since changes in neuronal firing and the accompanying release of neurotransmitters produce alterations at the molecular level [57], we analyzed the number of Fos-IR neurons within different cell groups associated with the LTPE effect to characterize distribution patterns of neuronal activity. Overall, Fos-IR neurons were concentrated mainly in the LDT/PPT, PBN, and L/MVN, and varied significantly as a function of postcarbachol days of LTPE (Fig. 4). For the cell groups of the LDT/PPT and L/MVN, the number of Fos-IR neurons was significantly higher than in controls, reaching a peak increase on day 03. The difference between the carbachol LTPE effect and controls was significant ($P < 0.0001$). Within individual nuclear regions of the PMT, these differences were statistically significant on day 03 for the LDT, in which the number of Fos-IR neurons (482.4 ± 29.8) reached a 40-fold increase (Fig. 4A), for the PPT, in which the number of Fos-IR neurons (551.7 ± 41.6) reached a 28-fold increase (Fig. 4B), and for the L/MVN, in which there was a 41-fold increase (190.6 ± 22.1; Fig. 4D), suggesting their involvement in maintaining the LTPE effect.

Conversely, the number of Fos-IR neurons surrounding the injection site in the PBN of the caudolateral PMT reached a 24-fold increase (288.7 ± 27.5) on day 01, followed by a significantly smaller number (31.2 ± 12.9) on day 03 (Fig. 4C). Since the expression of c-*fos* in the other cell groups remained high, the dramatic change in the activity of the PBN after day 01 suggests its involvement in the initiation of the LTPE effect.

We examined Fos-IR neurons outside of the PMT within limbic and subcortical regions whose physiological and state-dependent profiles have been shown to be involved in sleep–wake state behavior and in PGO control [59], but found very few Fos-IR neurons present in the CMN, DMN, DLN, and PLN of the hypothalamus, MHN of the thalamus, DG, CA3, CA1 cell groups of the hippocampus, and CN of the amygdala. Only a few Fos-IR neurons were seen in the LGN and pulvinar—two thalamic structures that participate actively in PGO wave neurophysiology [15,16]. These negative observations suggest that neurons involved in generating LTPE via cholinergically-induced c-*fos* expression are confined to the pontine brain stem.

4. Discussion

The principal finding of this study is that a single microinjection of carbachol nanospheres in the caudolateral PMT elicits LTPE and induces a striking, long-lasting increase in c-*fos* expression in the LDT/PPT matching the 5-day course of the LTPE effect. The results suggest that changes in gene expression may be a molecular correlate of the long-term enhancement of the phasic PGO component of REM sleep that is dissociated from other REM sleep signs and the rest of the behavioral state of sleep. To this point, we hypothesize that cholinergic activation at discrete sites within the caudolateral PMT alters the postsynaptic excitability of the PGO generator and potentiates the LTPE effect contributing to prolonged c-*fos* expression.

Since microinjection of carbachol-conjugated LNDS significantly limits diffusion of the drug, increased c-*fos* expression in the more rostral cell groups of the LDT/PPT suggests transsynaptic events that lead to c-*fos* transcription. We found this evidence of enduring Fos activity surprising because of the usually short-lived transient expression of Fos protein [28, 57] and reported downregulation of certain IEGs in the brain following acute pharmacological stimuli [33], albeit the mechanisms of c-*fos* downregulation remain obscure. This finding is of particular physiological relevance and importance to explain how a single micro-injection of drug leads to molecular changes at remote sites that persist for 5 days, long after the acute effects of the drug have disappeared.

It is noteworthy that phasic pontine wave (P-wave) activation during REM sleep has recently been shown to influence sleep-dependent learning [17,51], suggesting that P-wave activation enhances memory processes which occur normally during post-learning REM sleep [19].

Although we did not perform behavioral training or learning testing in this study, our findings of prolonged PGO enhancement and sustained expression of c-*fos* during sleep, but without REM sleep enhancement, extend the importance of studying the cellular and molecular mechanisms of the phasic events of REM sleep, including PGO activity and hippocampal theta frequency as possible indexes of information processing. Furthermore, LTPE may provide a new model system for exploration of intracellular pathways linking receptor activation to changes in gene expression and effector proteins involved in state-dependent plasticity and cognitive behavior [20,37,87].

4.1. Persistence of Fos immunoreactivity in the LDT/PPT cell groups

To our knowledge, this is the first study that demonstrates a sustained c-*fos* expression in response to pharmacological stimulation of the brain. In the usual time course of c-*fos* expression, transcriptional activation occurs within 5 min after even relatively short periods of stimulation and continues for 15–20 min [28]. Thereafter, mRNA accumulates and reaches peak values at 30–45 min post-stimulation followed by a decline with the relatively short half-life of approximately 12 min [57]. Fos protein is also relatively short-lived, with a half-life between 2 h and 6 h after an acute challenge returning to baseline control before 24 h [42, 56], as is typical of an intracellular signaling system.

Unlike the N-terminal antibody that we used in this study and that has been shown to be specific for c-*fos* [76,77], other M peptide antibodies have been shown to recognize epitopes shared between Fos and various Fos-related antigens (FRA). These FRA proteins are induced by stimuli similar to those that upregulate c-*fos*, but their expression peaks later and may last for 24–48 h [56,63,72,77]. Since we selected our primary antisera on the basis of its positive reactivity with the N-terminal domain (amino acids 2–16) and no known evidence of cross-reactivity with FRA, our discovery of c-*fos* expression lasting 5 days in the LDT/PPT following a single microinjection of cholinergic drug is unprecedented. This leads to our causal hypothesis that prolonged c-*fos* expression in the LDT/PPT has subsequent effects on long-term cellular adaptations coincident with the LTPE effect.

When viewed as messenger molecules, Fos functions in coupling short-term responses to external signals at the cell membrane to longer-term intracellular events, and in altering phenotype by regulating the expression of selected target and late response genes [28,56]. The specificity of the cellular response lies within the type of cell itself, and different target genes may be selected for regulation by c-*fos* in neurons of different neurotransmitter signatures [57]. Indeed, the rostral PMT cell groups of the LDT/PPT and the caudal PMT cell group of the PBN show a marked heterogeneity in PGO bursting properties and neurotransmitter populations [15,41,54,70,71,79,80,86]. We have taken an interest in these neurons and have shown that while cholinoceptive injection sites in the caudolateral PMT primarily receive cholinergic afferents from the LDT/PPT, non-cholinergic populations provide the greatest proportion of afferents [68]. This afferent circuitry may increase the efficacy of cholinoceptive synaptic transmission in the caudolateral PMT prompting a potentiation of PGO events that does not occur in normal REM.

The dramatic initial increase in c-*fos* expression on day 01 in the caudolateral PMT was followed by an equally striking decrease on day 03. Conversely, expression of c-*fos* continued to increase within the LDT/PPT. This difference in time course points toward a physiological dissociation between the cholinoceptive injection site in the caudolateral PMT and the more rostral cell groups of the LDT/PPT over the course of LTPE. While the functional consequences of such a dissociation have yet to be determined, one possibility is that the cellular response to overexpression of c-*fos* may be different in different cell types of the PMT. Alternatively, excitation of local circuitry in the caudolateral PMT leads to transsynaptic activation of the LDT/PPT that drives the LTPE effect and underlies the persistent expression of c-*fos*.

4.2. Molecular and network implications of regional c-fos expression

Our findings of an increase in the number of Fos-IR neurons in the L/MVN that paralleled the time course of the increase in phasic PGO wave clusters during LTPE suggest that L/MVN neurons are physiologically linked [27,64] and likely to synergize in the expression of c-*fos* with the LDT/PPT. PGO pontine pathways project through the tegmentum and communicate with the L/MVN, providing evidence, as do our results, of involvement of the vestibular system in the generation of PGO waves [58]. Additionally, there is agreement from physiological, pharmacological, and lesion studies that PGO-on neurons in the pontine tegmentum are considered to be the final transferring output components of the PGO generator network [15, 60,85]. This is a relevant point, since even dramatic conditions such as labyrinthectomy, that significantly changes the spontaneous firing rate of L/MVN neurons, do not modify c-*fos* expression in the L/MVN [12], whereas we find that LTPE does.

Interestingly, few Fos-IR neurons were seen in the FTG and throughout the other paramedian subdivisions of the pontine reticular formation in both controls and during LTPE, suggesting that these cell groups do not play a critical role in the LTPE effect. Neurons within this region have been extensively studied for their executive role in sleep–wake behavioral state control [1,78] and have been shown to be a source of net excitatory drive with reciprocal connections to cholinergic cell groups of the PMT [44,80]. Our recent anatomical studies of LDT/PPT neurons during LTPE reveal the presence of cholinergic, gamma-amino-butyric acid (GABA)-ergic, and glutamatergic transmitter phenotypes [29] and reciprocity between Fos-IR projection neurons and injection sites in the caudolateral PMT [30]. These results suggest that the PMT has the local network connections needed to maintain the LTPE effect. Based on these observations, we take the view that the few Fos-IR neurons in the FTG add credence to our original suggestion of the paramedian pontine reticular formation being a trigger zone for REM while the caudolateral PMT acts as a regulatory region capable of inducing the LTPE effect long after the acute effects of carbachol have disappeared [34,65].

The finding of few Fos-IR neurons in the posterior hypothalamic cell groups of the CMN, DLN, DMN, and PLH, the MHN, the DG, CA3, and CA1 subdivisions of the hippocampus, and the CN of the amygdala in controls and during successive days of LTPE stands in clear contrast to the neurons of the PMT that were quantified, making molecular support for involvement of these other cell groups in LTPE less clear. Since it is known that neurons may be activated but with no evidence of Fos-IR labeling [21], the absence of Fos immunoreactivity does not necessarily indicate the absence of a response. We interpreted Fos immunoreactivity as an indicator of neuronal activation in the soma and not in axon/dendrites, which can be detected by 2-deoxyglucose (2-DG) uptake [21,23]. A systems level interpretation is that the few FosIR neurons within these remote brain regions play an integrative role in orchestrating the network facilitation of LTPE and may also be a significant predictor of PGO enhancement [6,59,83]. Many Fos-IR cells have been found in limbic structures of the dorsal hippocampus, amygdala, and nuclei of the basal forebrain associated with enhanced sleep–wake states following microinjection of muscimol into the periaqueductal gray [75]. The expression of c-*fos* in these areas is suggested as a tonic component of REM sleep at the molecular level. Since PGO enhancement is a self-sustaining and long-term, phasic behavior, neurons in these areas do not appear to be the primary neurons of the LTPE effect. Our findings of LTPE, but without REM enhancement, indicate that the PGO generator can be dissociated from the REM sleep network, suggesting that the PGO circuitry does not necessarily recruit REM sleep generator neurons and may not exert a proportionate priming influence on REM sleep enhancement. Alternatively, the state of excitation in these subcortical and limbic cell groups during LTPE may involve transcriptional regulators other than c-*fos* and induction mechanisms different from those within the LDT/PPT that are not necessarily involved in REM sleep, thereby restricting the transcription of specific genes such as c-*fos* during LTPE.

Although the present study does not suggest a mechanism by which LTPE may preferentially increase the c-*fos* response of the caudolateral PMT and LDT/PPT cell groups without influencing subcortical and limbic regions, recent work points to dominant intracellular pathways involving cyclic AMP (cAMP) and the association of signaling molecules with calcium channels that are more likely to induce a response than other pathways [35,89]. Our thinking is that multiple gene pathways may be associated with the LTPE effect.

It is not clear how a differential distribution of the number of Fos-IR neurons among discrete PMT and subcortical cell groups could be the result of a cholinoceptive local network activation originating in the caudolateral PMT. This question of the functional relationship between c-*fos* expression and LTPE is in the center of discussion and in need of a comparative mapping of interactions among other IEGs of c-*Jun*, *jun-B*, *fosB*, *egr-1*, and of transduction pathways involving activation of the cAMP-dependent protein kinase (PKA) cascade with subsequent activation of the cAMP response element-binding protein (CREB) [14]. At the same time, there are questions of causality. Primarily, which events trigger the recruitment of c-*fos* activity that so closely parallels the time course of LTPE? Furthermore, how do changes in gene expression mediate state-dependent modifications in neural activity within large populations of neurons to produce cell-specific, long-term responses [32,36,55]? Given the importance of determining whether the mechanism of sustained c-*fos* expression during LTPE is attributed to cause rather than effect, we see the potential of functional genomics and proteomics to develop more refined drug delivery methods. The use of effective small interfering RNA (siRNA) gene silencing and the discovery of additional target genes will allow a better understanding of the network pathways and mechanisms of action that are utilized to activate neurons involved in the LTPE effect. Moreover, we reason that the limited diffusion properties of carbachol-conjugated LNDS are well suited to such investigations of cellular and molecular controls and will illuminate future strategies in comparing the spread of cholinergic excitation at spatially discrete PMT sites that produce long-term behavioral state effects.

4.3. Concluding remarks

The LTPE effect offers a model system to study the molecular switches by which gene expression in response to acute drug treatment leads to long-term changes in brain regulatory systems. This conceptual framework helps us design studies that integrate cellular, synaptic, and network modalities of tonic/phasic excitability underlying PGO generation [31] and understand how molecular changes in the downstream targets of IEGs affect long-term neuromodulation of brain state control. Given recent findings that sleep and mechanisms of neural plasticity appear to share molecular pathways [13], the study of sleep may answer the future challenge to characterize the precise molecular steps leading to the changes in brain activity of drug abuse, anxiety, depression, and addiction. Since sleep architecture is disrupted in all of these conditions, we expect our findings to be valuable in understanding these long-term pathologies.

Acknowledgments

This work was supported in part by NIH Grants HL-72702 and MH-13923. We thank J. Beck, C. Cirelli, M. Greenberg, W. Ham, B. Kocsis, C. Saltzman, T. Scammell, and M.T. Tsuang for helpful comments and discussion; R. Buzescu, P. Goldhoff, A. Heilman, R.T. Lau, A. Mostaghimi, R. Moreno, A. Nathoo, K. Rowe, J. Su, R. Verrier, and M. Wilcox for technical assistance; and P. Koretsky, A. Lage, W. Liddell, J. Pettit, and A. Warner for surgical assistance and veterinary care.

References

1. Baghdoyan, HA. Cholinergic mechanisms regulating REM sleep. In: Schwartz, WJ., editor. Sleep Science: Integrating Basic Research and Clinical Practice, Monogr. Clin. Neurosci. 15. Krager; Basel: 1997. p. 88-116.

2. Baghdoyan, HA.; McCarley, RW.; Hobson, JA. Cholinergic manipulation of brain stem reticular systems: effects on REM sleep generation. In: Wauquier, A.; Gaillard, JM.; Monti, JM.; Radulovacki, M., editors. Sleep: Neurotransmitters and Neuromodulators. Raven Press; New York: 1985. p. 15-27.
3. Baghdoyan HA, Lydic R, Callaway CW, Hobson JA. The carbachol-induced enhancement of desynchronized sleep signs is dose-dependent and antagonized by centrally administered atropine. Neuropsychopharmacology 1989;2:67–79. [PubMed: 2572234]
4. Berman, AL. The Brain Stem of the Cat. Wisconsin Press; Madison: 1968.
5. Buller KM, Allen T, Wilson LD, Munro F, Day TA. A critical role for the parabrachial nucleus in generating central nervous system responses elicited by a systemic immune challenge. J. Neuroimmunol 2004;152:20–32. [PubMed: 15223234]
6. Buzsaki G, Draguhn A. Neuronal oscillations in cortical networks. Science 2004;304:1926–1929. [PubMed: 15218136]
7. Callaway C, Lydic R, Baghdoyan HA, Hobson JA. PGO waves: spontaneous visual system activity during REM sleep. Cell. Mol. Neurobiol 1987;7:105–149. [PubMed: 3308096]
8. Cirelli C, Tononi G. Differences in brain gene expression between sleep and waking as revealed by mRNA differential display and cDNA microarray technology. J. Sleep Res 1999;8:44–52. [PubMed: 10389106]
9. Cirelli C, Tononi G. On the functional significance of c-*fos* induction during the sleep–waking cycle. Sleep 2000;23:453–469. [PubMed: 10875553]
10. Cirelli C, Pompeiano M, Tononi G. Sleep deprivation and c-*fos* expression in the rat brain. J. Sleep Res 1995;4:92–106. [PubMed: 10607147]
11. Cirelli C, Pompeiano M, Tononi G. Neuronal gene expression in the waking state: a role for the locus coeruleus. Science 1996;274:1211–1215. [PubMed: 8895474]
12. Cirelli C, Pompeiano M, D'Ascanio P, Arrighi P, Pompeiano O. C-fos expression in the rat brain after unilateral labyrinthectomy and its relation to the uncompensated and compensated stages. Neuroscience 1996;70:515–546. [PubMed: 8848156]
13. Cirelli C, Gutierrez CM, Tononi G. Extensive and divergent effects of sleep and wakefulness on brain gene expression. Neuron 2004;41:35–43. [PubMed: 14715133]
14. Cole RL, Konradi C, Douglass J, Hyman SE. Neuronal adaptation to amphetamine and dopamine: molecular mechanisms of prodynorphin gene regulation in rat striatum. Neuron 1995;14:813–823. [PubMed: 7718243]
15. Datta S. Cellular basis of PGO wave generation and modulation. Cell. Mol. Neurobiol 1997;17:341–365. [PubMed: 9187490]
16. Datta, S. PGO wave generation: mechanism and functional significance. In: Mallick, BN.; Inoue, S., editors. Rapid Eye Movement Sleep. Narosa; New Delhi: 1999. p. 91-106.
17. Datta S. Avoidance task training potentiates phasic pontine-wave density in the rat: a mechanism for sleep-dependent plasticity. J. Neurosci 2000;20:8607–8613. [PubMed: 11069969]
18. Datta S, Calvo J, Quattrochi J, Hobson JA. Long-term enhancement of REM sleep following cholinergic stimulation. NeuroReport 1991;2:619–622. [PubMed: 1756243]
19. Datta S, Mavanji V, Ulloor J, Patterson EH. Activation of phasic pontine-wave generator prevents rapid eye movement sleep deprivation-induced learning impairment in the rat: a mechanism for sleep-dependent plasticity. J. Neurosci 2004;24:1416–1427. [PubMed: 14960614]
20. Dragunow M. A role for immediate-early transcription factors in learning and memory. Behav. Genet 1996;26:293–299. [PubMed: 8754252]
21. Dragunow M, Faull R. The use of c-*fos* as a metabolic marker in neuronal pathway tracing. J. Neurosci. Methods 1989;29:261–265. [PubMed: 2507830]
22. Dunan RS, Heninger GR, Nestler EJ. A molecular and cellular theory of depression. Arch. Gen. Psychiatry 1997;54:597–606. [PubMed: 9236543]
23. Eells JB, Clough RW, Miller JW, Jobe PC, Browning RA. Fos expression and 2-deoxyglucose uptake following seizures in developing genetically epilepsy-prone rats. Brain Res. Bull 2000;52:379–389. [PubMed: 10922517]

24. El Mansari M, Sakai K, Jouvet M. Unitary characteristics of presumptive cholinergic tegmental neurons during the sleep–waking cycle in freely moving cats. Exp. Brain Res 1989;76:519–529. [PubMed: 2551709]
25. Freedman R. Long-term effects of early genetic influences on behavior. N. Engl. J. Med 2002;347:213–215. [PubMed: 12124413]
26. Garcia-Rill E. The pedunculopontine nucleus. Prog. Neurobiol 1991;36:363–389. [PubMed: 1887068]
27. Ghelarducci B, Pompeiano O. Oscillatory potentials in the lateral geniculate nucleus during sleep and wakefulness. Arch. Ital. Biol 1971;109:37–58. [PubMed: 4326765]
28. Greenberg M. Regulation and function of c-*fos* and other EGS in the nervous system. Neuron 1990;37:477–485. [PubMed: 1969743]
29. Ham W, Quattrochi J. Molecular mapping of the PGO generator network. Neurosci. Abstrs 2004;30:764.
30. Heilman A, Quattrochi J. C-fos expression of mesopontine reciprocal connectivity during carbachol induced long-term PGO enhancement (LTPE). Neurosci. Abstr 2002;27:599.
31. Heilman A, Quattrochi J. Simulations of PGO wave generation: integration of cholinergic and GABA-ergic feedback mechanisms with Cat and network dynamics at multiple levels. Neurosci. Abstr 2004;30:517.
32. Herdegen T, Leah JD. Inducible and constitutive transcription factors in the mammalian nervous system: control of gene expression by Jun, Fos, Krox, and CREB/ATF proteins. Brain Res. Rev 1998;28:370–490. [PubMed: 9858769]
33. Herrara DG, Robertson HA. Activation of c-*fos* in the brain. Prog. Neurobiol 1996;50:83–107. [PubMed: 8971979]
34. Hobson JA, Datta S, Calvo JM, Quattrochi J. Acetylcholine as a brain state modulator: triggering and long-term regulation of REM sleep. Prog. Brain Res 1993;98:389–404. [PubMed: 8248527]
35. Hoffman GE, Lyo D. Anatomical markers of activity in neuroendocrine systems: are we all “fos-ed” out? J. Neuroendrocrinol 2002;14:259–268.
36. Hughes PE, Dragunow M. Induction of immediate early genes and the control of neurotransmitter-regulated gene expression within the nervous system. Pharmacol. Rev 1995;47:134–178.
37. Hughes PE, Alexi T, Walton M, Williams CE, Dragunow M, Clark RG, Gluckman PD. Activity and injury-dependent expression of inducible transcription factors, growth factors and apoptosis-related genes within the central nervous system. Prog. Neurobiol 1999;57:421–450. [PubMed: 10080384]
38. Hyman SE. Genes, gene expression, and behavior. Neurobiol. Dis 2000;7:528–532. [PubMed: 11042069]
39. Hyman SE. Mental illness: genetically complex disorders of neural circuitry and neural communication. Neuron 2000;28:321–323. [PubMed: 11144341]
40. Hyman SE, Malenka RC. Addiction and the brain: the neurobiology of compulsion and its persistence. Nat. Rev., Neurosci 2001;2:695–703. [PubMed: 11584307]
41. Jones BE, Beaudet A. Distribution of acetylcholine and catecholamine neurons in the cat brain studied by choline acetyl transferase and tyrosine hydroxylase immunohistochemistry. J. Comp. Neurol 1987;261:15–32. [PubMed: 2887593]
42. Kaczmarek, L.; Robertson, HA. Immediate early genes and inducible transcription factors in mapping of the central nervous system function and dysfunction. In: Bjorklund, A.; Hokfelt, T., editors. Handb. Chem. Neuroanat. 19. Elsevier; Amsterdam: 2002.
43. Kamondi A, Williams JA, Hutcheon B, Reiner PB. Membrane properties of mesopontine cholinergic neurons studied with the whole-cell patch-clamp technique: implications for behavioral state control. J. Neurophysiol 1992;68:1359–1372. [PubMed: 1359028]
44. Leonard CS, Llinas R. Serotonergic and cholinergic inhibition of mesopontine cholinergic neurons controlling REM sleep: an in vitro electrophysiological study. Neuroscience 1994;59:309–330. [PubMed: 8008195]
45. Lin JS, Hou Y, Sakai K, Jouvet M. Histaminergic descending inputs to the mesopontine tegmentum and their role in the control of cortical activation and wakefulness in the cat. J. Neurosci 1996;16:1523–1537. [PubMed: 8778302]

46. Macklis JD, Quattrochi J. Restricted diffusion and stability of carbachol-fluorescent nanospheres in vivo. NeuroReport 1991;2:247–250. [PubMed: 1912455]
47. Maloney KJ, Mainville L, Jones BE. Differential c-*fos* expression in cholinergic, monoaminergic, and GABAergic cell groups of the pontomesencephalic tegmentum after paradoxical sleep deprivation and recovery. J. Neurosci 1999;19:3057–3072. [PubMed: 10191323]
48. Mamelak A, Quattrochi J, Hobson JA. A microcomputer-based system for automated EEG collection and scoring of behavioral state. Brain Res. Bull 1988;21:843–849. [PubMed: 3219615]
49. Mamelak A, Quattrochi J, Hobson JA. Automated staging of sleep using neural networks. Electroencephalogr. Clin. Neurophysiol 1991;79:52–61. [PubMed: 1713552]
50. Manaye KF, Zweig R, Wu D, Hersh LB, De Lacalle S, Saper CB, German DC. Quantification of cholinergic and select noncholinergic mesopontine neuronal populations in the human brain. Neuroscience 1999;89:759–770. [PubMed: 10199611]
51. Mavanji V, Datta S. Activation of the phasic pontine-wave generator enhances improvement of learning performance: a mechanism for sleep-dependent plasticity. Eur. J. Neurosci 2003;17:359–370. [PubMed: 12542673]
52. Merchant-Nancy H, Vasquez J, Aguilar-Roblero R. C-fos protooncogene changes in relation to REM sleep duration. Brain Res 1992;579:342–346. [PubMed: 1628220]
53. Mesulam, MM. Central cholinergic pathways: neuroanatomy and some behavioral implications. In: Avoli, M.; Reader, T.; Dykes, R., editors. Neurotransmitters and Cortical Function. Plenum; 1988. p. 237-260.
54. Mesulam MM, Geula C, Bothwell MA, Hersh L. Human reticular formation: cholinergic neurons of the PPT and LDT nuclei and some cytochemical comparisons to forebrain cholinergic neurons. J. Comp. Neurol 1989;283:611–633. [PubMed: 2545747]
55. Moratalla R, Elibol B, Vallejo M, Braybiel AM. Network-level changes in expression of inducible fos–jun proteins in the striatum during chronic cocaine treatment and withdrawal. Neuron 1996;17:147–156. [PubMed: 8755486]
56. Morgan J, Curran T. Stimulus transcription coupling in neurons: role of cellular immediate-early genes. Trends Neurosci 1989;12:459–462. [PubMed: 2479148]
57. Morgan J, Curran T. Stimulus-transcription coupling in the nervous system: involvement of the inducible proto-oncogenes fos and jun. Annu. Rev. Neurosci 1991;14:421–451. [PubMed: 1903243]
58. Morrison AR, Pompeiano O. Vestibular influences during sleep. Arch. Ital. Biol 1966;104:425–458. [PubMed: 5982752]
59. Morrison, AR.; Sanford, LD.; Ross, RJ. Initiation of rapid eye movement sleep: beyond the brainstem. In: Mallick, BN.; Inoue, S., editors. Rapid Eye Movement Sleep. Narosa; New Delhi: 1999. p. 51-68.
60. Nelson JP, McCarley R, Hobson JA. REM sleep burst neurons, PGO waves, and eye movement information. J. Neurophysiol 1983;50:784–797. [PubMed: 6631463]
61. Nestler EJ. Genes and addiction. Nat. Genet 2000;26:277–281. [PubMed: 11062465]
62. Nestler EJ. Molecular basis of long-term plasticity underlying addiction. Nat. Rev., Neurosci 2001;2:119–128. [PubMed: 11252991]
63. Nestler EJ, Barrot M, Self DW. ΔFos B: a sustained molecular switch for addiction. Proc. Natl. Acad. Sci 2001;98:11042–11046. [PubMed: 11572966]
64. Pompeiano O, Morrison AR. Vestibular influences during sleep. I. Abolition of the rapid eye movements during desynchronized sleep following vestibular lesions. Arch. Ital. Biol 1965;103:569–595. [PubMed: 5867666]
65. Quattrochi, J.; Hobson, JA. Carbachol-fluorescent microspheres: a new method for behavioral neurobiology. In: Mancia, M.; Marini, G., editors. The Diencephalon and Sleep. Raven Press; New York: 1990. p. 65-76.
66. Quattrochi J, Hobson JA. Carbachol microinjection into the caudal peribrachial area induces long-term enhancement of PGO wave activity but not REM sleep. J. Sleep Res 1999;8:281–290. [PubMed: 10646168]
67. Quattrochi J, Mamelak A, Madison R, Macklis JD, Hobson JA. Mapping neuronal inputs to REM sleep induction sites with carbachol-fluorescent microspheres. Science 1989;245:984–986. [PubMed: 2475910]

68. Quattrochi J, Datta S, Hobson JA. Cholinergic and noncholinergic afferents of the caudolateral parabrachial nucleus: a role in the long-term enhancement of REM sleep. Neuroscience 1998;83:1123–1136. [PubMed: 9502251]
69. Reese NB, Garcia-Rill E, Skinner RD. The pedunculopontine nucleus-auditory input, arousal and pathophysiology. Prog. Neurobiol 1995;42:105–133. [PubMed: 8711130]
70. Reiner PB, Vincent SR. Topographic relations of cholinergic and noradrenergic neurons in the feline pontomesencephalic tegmentum: an immunohistochemical study. Brain Res. Bull 1987;19:705–714. [PubMed: 2894238]
71. Rye DB. Contributions of the pedunculopontine region to normal and altered REM sleep. Sleep 1997;20:757–788. [PubMed: 9406329]
72. Sagar SM, Sharp FR, Curran T. Expression of c-*fos* protein in brain: metabolic mapping at the cellular level. Science 1988;240:1328–1331. [PubMed: 3131879]
73. Saito H, Sakai K, Jouvet M. Discharge patterns of the nucleus parabrachialis lateralis neurons of the cat during sleep and waking. Brain Res 1977;134:59–72. [PubMed: 912422]
74. Samaha A-N, Mallet N, Ferguson S, Gonon F, Robinson TE. The rate of cocaine administration alters gene regulation and behavioral plasticity: implications for addiction. J. Neurosci 2004;24:6362–6370. [PubMed: 15254092]
75. Sastre JP, Buda C, Lin JS, Jouvet M. Differential c-*fos* expression in the rhinencephalon and striatum after enhanced sleep–wake states in the cat. Eur. J. Neurosci 2000;12:1397–1410. [PubMed: 10762368]
76. Scammell T, Gerashchenko D, Urade Y, Onoe H, Saper CB, Hayaishi O. Activation of ventrolateral preoptic neurons by the somnogen prostaglandin D2. Proc. Natl. Acad. Sci 1998;95:7754–7759. [PubMed: 9636223]
77. Schilling E, Curran T, Morgan J. The excitement of immediate-early genes. Ann. N. Y. Acad. Sci 1991:115–121. [PubMed: 1909106]
78. Semba K. Aminergic and cholinergic afferents to REM sleep induction regions of the pontine reticular formation in rat. J. Comp. Neurol 1993;330:543–556. [PubMed: 7686567]
79. Semba, K. The mesopontine cholinergic system: a dual role in REM sleep and wakefulness. In: Lydic, R.; Baghdoyan, HA., editors. Handbook of Behavioral State Control: Cellular and Molecular Mechanisms. CRC Press; New York: 1999. p. 161-180.
80. Semba K, Fibiger HC. Afferent connections of the laterodorsal and pedunculopontine tegmental nuclei in the rat: a retro- and antero-grade transport and immunohistochemical study. J. Comp. Neurol 1992;322:1–24. [PubMed: 1430305]
81. Sherin JE, Shiromani PJ, McCarley RW, Saper CB. Activation of ventrolateral preoptic neurons during sleep. Science 1996;271:216–218. [PubMed: 8539624]
82. Shiromani PJ, Winston S, McCarley RW. Pontine cholinergic neurons show fos-like immunoreactivity associated with cholinergically induced REM sleep. Mol. Brain Res 1996;38:77–84. [PubMed: 8737670]
83. Simon-Arceo K, Ramirez-Salado I, Calvo JM. Long-lasting enhancement of rapid eye movement sleep and pontogeniculooccipital waves by vasoactive intestinal peptide microinjection into the amygdala temporal lobe. Sleep 2003;26:259–264. [PubMed: 12749543]
84. Sommer W, Rimondini R, O'Connor W, Hansson AC, Ungerstedt U, Fuxe K. Intrastriatally injected c-*fos* antisense oligonucleotide interferes with striatonigral but not striatopallidal γ-amino-butyric acid transmission in the conscious rat. Proc. Natl. Acad. Sci. U. S. A 1996;93:14134–14139. [PubMed: 8943073]
85. Steriade M, Pare D, Datta S, Oakson G, Currodossi R. Different cellular types in mesopontine cholinergic nuclei related to PGO waves. J. Neurosci 1990;10:2560–2579. [PubMed: 2201752]
86. Vincent SR, Reiner PB. The immunohistochemical localization of choline acetyltransferase in the cat brain. Brain Res. Bull 1987;18:371–415. [PubMed: 3555712]
87. Walton M, Henderson C, Mason-Parker S, Lawlor P, Abraham WC, Bilkey D, Dragunow M. Immediate early gene transcription and synaptic modulation. J. Neurosci. Res 1999;58:96–106. [PubMed: 10491575]

88. Webster HH, Jones BE. Neurotoxic lesions of the dorsolateral pontomesencephalic tegmentum cholinergic cell area in the cat, II. Effects upon sleep–waking states. Brain Res 1988;458:285–302. [PubMed: 2905197]

89. West AE, Chen WG, Dalva M, Dolmetsch R, Kornhauser J, Shaywitz A, Takasu M, Tao X, Greenberg ME. Calcium regulation of neuronal gene expression. Proc. Natl. Acad. Sci. U. S. A 2001;98:11024–11031. [PubMed: 11572963]

90. Yamuy J, Mancillas J, Morales F, Chase MH. C-fos expression in the pons and medulla of the cat during carbachol induced active sleep. J. Neurosci 1993;13:2703–2718. [PubMed: 8501533]

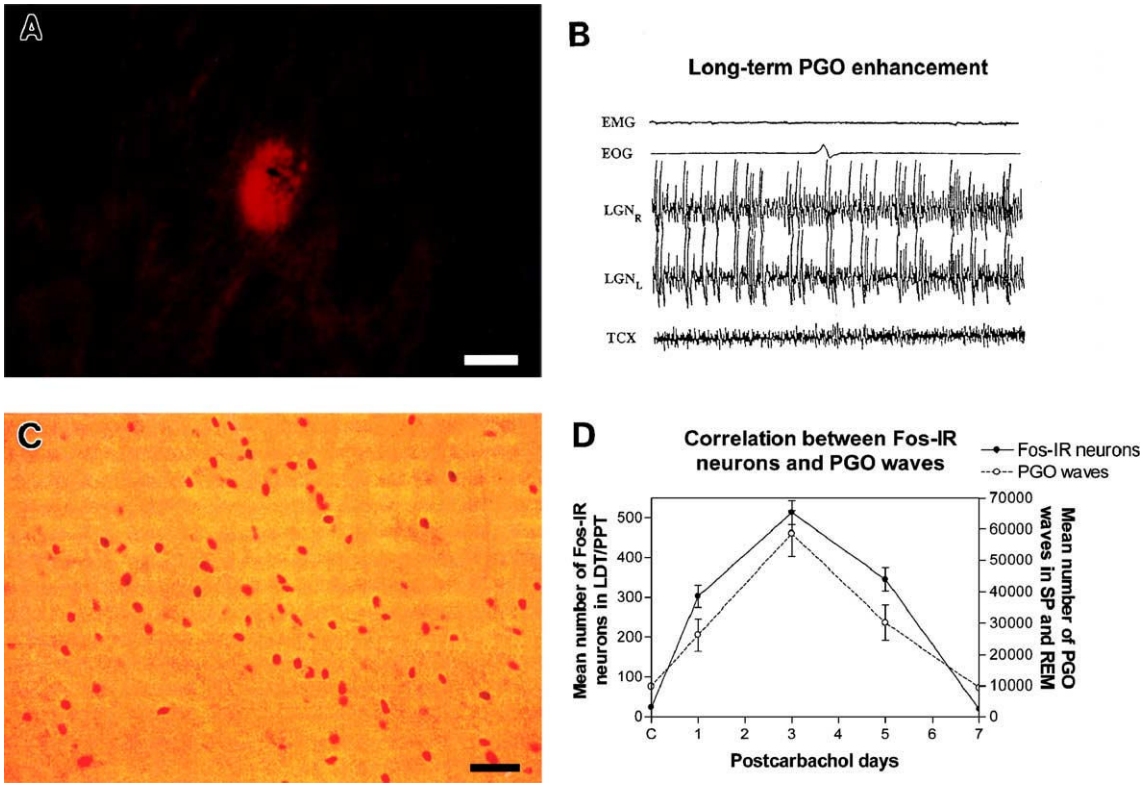

Fig. 1.

Carbachol-induced long-term PGO enhancement (LTPE) and Fos immunoreactivity (Fos-IR). (A) Fluorescent photomicrograph of a rhodamine nanosphere injection site is shown in one representative case on day 01 of the LTPE effect. Injection site is located ventral to the inferior margin of the brachium conjunctivum in the caudolateral pontomesencephalic tegmentum (PMT, P3.6, L4.5, H-2.5). Injection site has a mean diameter of 91.3 μm. Scale bar, 50 μm. (B) Polygraphic record of REM sleep on day 03 of LTPE following a single unilateral carbachol microinjection in the caudolateral PMT shows increased frequency of bilateral PGO waves. (C) Photomicrograph of Fos-IR neurons within the PPT on postcarbachol day 03. Scale bar, 50 μm. (D) Graphs represent mean number of Fos-IR neurons quantified in the LDT/PPT and the mean number of PGO waves quantified on successive postcarbachol days during LTPE. Data demonstrate increased numbers of Fos-IR neurons correlated with intensity and time course of the LTPE effect. $r^2 = 0.85$.

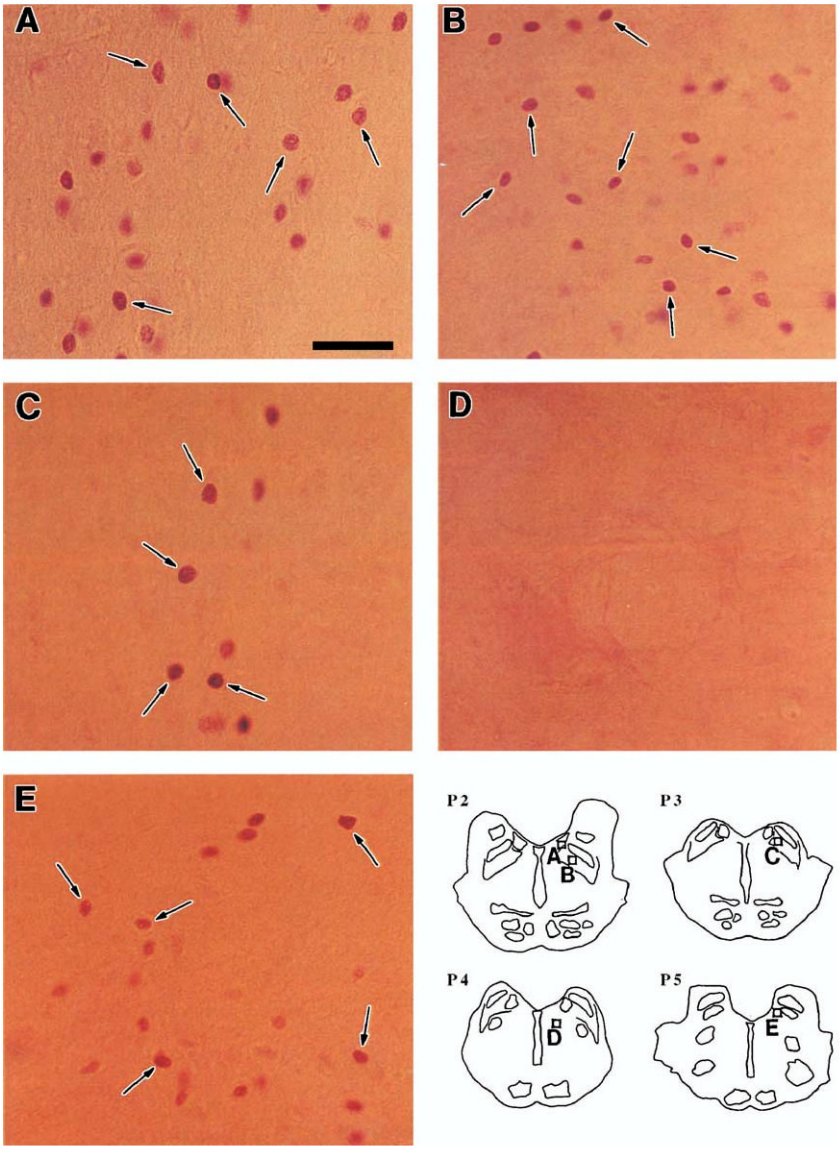

Fig. 2.

Photomicrographs of Fos-IR neurons (arrows) on postcarbachol day 03 of the LTPE effect. (A) LDT, (B) PPT, (C) PBN, (D) FTG (note the lack of Fos-IR neurons), (E) MVN. Scale bar, 50 μm. Inset: Schematic transverse sections (P2.0–P5.0) identify nuclear regions of micrographs A–E.

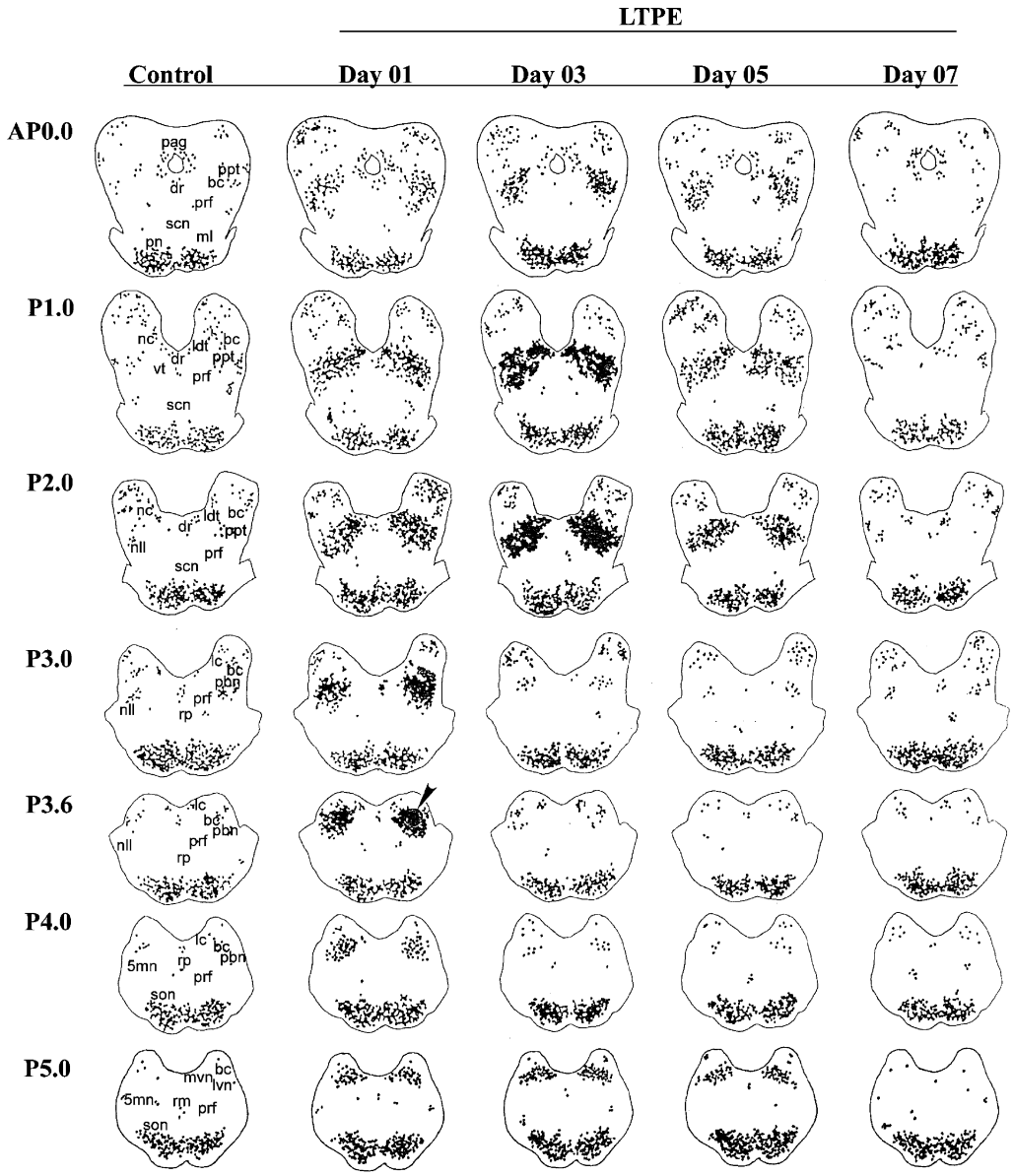

Fig. 3.

Time course and rostrocaudal distribution of Fos-IR neurons following a single carbachol nanosphere microinjection. Drug injection site is shown at level P3.6 (arrowhead) on day 01. Fos-IR neurons are seen in one representative control and during LTPE on each postcarbachol day 01, 03, 05, and 07. Each point represents one Fos-IR neuron. 5mn, trigeminal motor nucleus; bc, brachium conjunctivum; ldt, laterodorsal tegmental nucleus; dr, raphe dorsalis; lc, locus coeruleus; lvn, lateral vestibular nucleus; ml, medial lemniscus; mvn, medial vestibular nucleus; nc, nucleus cuneiformis; nll, nucleus lateral lemniscus; pag, periaqueductal gray; pbn, parabrachial nucleus; pn, pontine nuclei; ppt, pedunculopontine tegmental nucleus; prf, pontine reticular formation; rm, raphe magnus; rp, raphe pontis; scn, superior central nucleus; son, superior olivary nucleus; vt, ventral tegmentum.

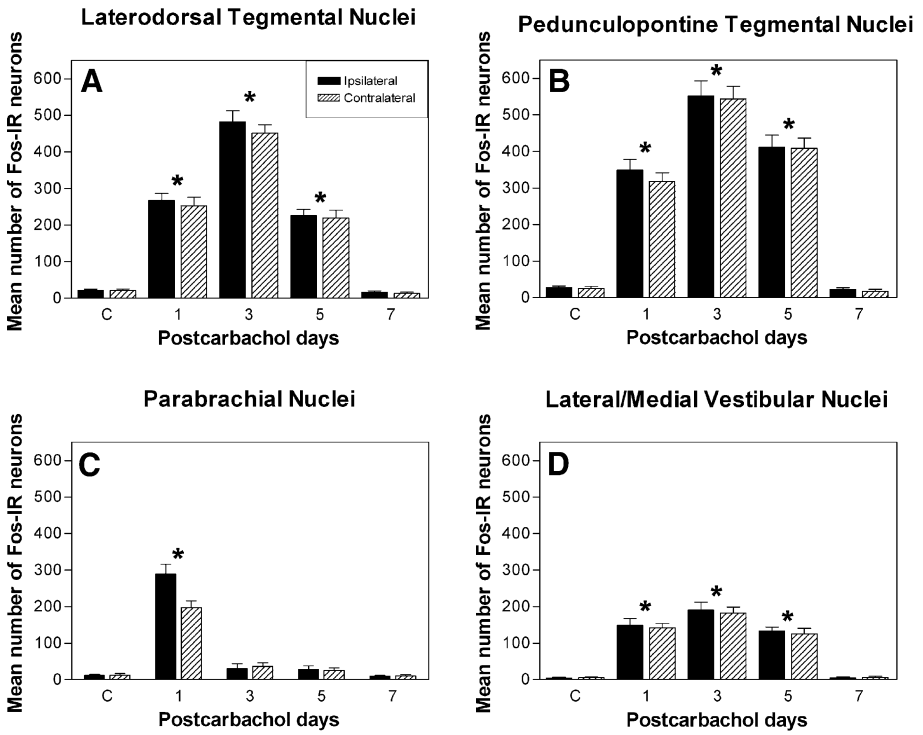

Fig. 4.

Mean number of Fos-IR neurons within nuclear regions of the pontomesenphalic tegmentum (PMT) in controls and during postcarbachol days 01, 03, 05, and 07 of LTPE. (A) LDT, (B) PPT, (C) PBN, (D) L/MVN. The number of Fos-IR neurons within the vicinity of the drug injection site in the PBN increases only on day 01 (*$P < 0.0001$) followed by a decrease over the course of the LTPE effect. Conversely, the number of Fos-IR neurons in the LDT, PPT, and L/MVN increases after day 01 reaching a peak on day 03 (*$P < 0.0001$). This distinctly different distribution and time course of Fos-IR neurons is also seen in Fig. 3. There are significantly more Fos-IR neurons ipsilateral to the microinjection site in the PBN and only on day 01. In all other cell groups, there is no significant difference ($P > 0.05$) in the number of Fos-IR neurons between ipsilateral and contralateral regions.

Table 1

Effects on sleep - wake states and PGO waves following a single microinjection of carbachol nanospheres in the caudolateral pontomesencephalic tegmentum

Baseline (*n* = 16)		**W**	**SWS**	**SP**	**REM**	**PGO**	**Postinjection hours to perfusion**
		43.5 (7.2)	**30.1 (5.6)**	**5.9 (2.5)**	**20.6 (3.3)**	**9759.2 (423.5)**	
Control (*n* = 4)	Day 01	42.3	34.1	6.2	17.4	9965.0	4.4
	Day 03	39.1 (3.2)	38.7 (4.6)	6.5 (0.3)	18.4 (1.1)	10659.5 (563.3)	52.5
	Day 05	38.1 (2.5)	36.3 (3.4)	6.6 (0.5)	18.8 (0.9)	10426.7 (517.8)	100.4
	Day 07	40.1 (2.3)	35.8 (2.1)	7.1 (0.3)	18.3 (0.9)	11279.3 (616.3)	148.4
Carbachol (*n* = 12)	Day 01	39.1 (7.9)	36.3 (4.9)	7.4 (3.1)	17.6 (3.7)	26188.5 (5078.7)*	4.5 (0.05)
	Day 03	37.6 (6.8)	35.7 (5.6)	6.6 (3.4)	18.3 (4.2)	58618.3 (7358.5)*	52.4 (0.07)
	Day 05	35.9 (7.8)	41.5 (6.2)	5.3 (3.7)	15.4 (3.7)	30135.8 (5597.2)*	100.4 (0.06)
	Day 07	44.6 (8.2)	32.9 (5.5)	7.1 (4.2)	18.1 (4.7)	9329.6 (631.5)	148.5 (0.03)

Results of sleep–wake states are shown as mean percentage (±SEM) of 4-h recording time. PGO state is expressed as the number of PGO waves (±SEM) in SP and REM. Days 01, 03, 05, 07 are designated by postinjection hours (±SEM) to perfusion (W, wakefulness; SWS, slow wave sleep; SP, slow wave sleep with PGO; REM, rapid eye movement sleep; PGO, ponto-geniculo-occipital waves).

* $P < 0.001$.